Jialong Chen, Quanli Li, Jianguang Xu, Le Zhang, Manfred F. Maitz, Jun Li

Thromboresistant and rapid-endothelialization effects of dopamine and staphylococcal protein A mediated anti-CD34 coating on 316L stainless steel for cardiovascular devices

Erstveröffentlichung in / First published in:
Journal of Materials Chemistry B. 2015, 3(13), S. 2615 - 2623 [Zugriff am: 04.11.2019]. Royal Society of Chemistry. ISSN 2050-7518.

DOI: https://doi.org/10.1039/c4tb01825g

Journal of Materials Chemistry B

PAPER

View Article Online
View Journal | View Issue

Cite this: J. Mater. Chem. B, 2015, 3, 2615

Thromboresistant and rapid-endothelialization effects of dopamine and staphylococcal protein A mediated anti-CD34 coating on 316L stainless steel for cardiovascular devices

Jialong Chen,*[ab] Quanli Li,[a] Jianguang Xu,[a] Le Zhang,[a] Manfred F. Maitz[c] and Jun Li*[b]

Received 5th November 2014
Accepted 26th January 2015

DOI: 10.1039/c4tb01825g

www.rsc.org/MaterialsB

There is convincing evidence *in vivo* that the vascular homing of endothelial progenitor cells (EPCs) contributes to rapid endothelial regeneration, which could prevent thrombosis and restenosis of cardiovascular devices. To enhance the EPC homing on cardiovascular devices, immobilization of an EPC capture agent (*e.g.* an anti-CD34 antibody) on the surface of cardiovascular devices is critical. We describe a way of immobilizing anti-CD34 Ab on 316L Stainless Steel (316L SS). For this, surface modification of 316L SS was performed *via* self-polymerization of dopamine (DA) and covalent grafting of staphylococcal protein A (SPA). On this coating the anti-CD34 Abs were oriented immobilized through their Fc constant region with SPA. In this process, the results of quartz crystal microbalance, X-ray photoelectron spectroscopy and water contact angle studies indicate that DA, SPA and anti-CD34 Ab were successfully immobilized onto the surface step by step. *In vitro* blood-compatibility tests confirmed that the modified surface induced less pro-coagulant fibrinogen denaturation, less platelet adhesion and lower activation of the adherent platelets. The affinity of EPCs for the modified surface has been demonstrated under flow conditions. This study provides potential applications for cardiovascular implant materials.

1. Introduction

Many cardiovascular and other blood contacting biomedical devices have been widely applied, such as vascular stents, vascular grafts, artificial heart valves, or blood pumps,[1] and contribute significantly to the quality and effectiveness of the health care system. However, in the environment of blood, complications such as blood clotting and thrombus formation or, in the case of vascular stents, proliferation of smooth muscle cells and restenosis frequently lead to the failure of the device. Surface engineering is required to provide improved passive or active hemocompatible properties.[2]

Permanent medical devices in the blood stream are prone to thrombus formation on their surface, which hinders rapid and complete coverage of the device by endothelial cells (ECs). ECs, physiologically the inner lining of blood vessels, are desired to colonize a biomedical device, because they exhibit anticoagulant and anti-adhesive properties for blood platelets and leukocytes.[3]

Restenosis is a direct consequence of vessel injury during stent implantation, fibrin deposition, infiltration with inflammatory cells with subsequent neointima formation and remodeling resulting in occlusion of the lumen.[3] These developments result from a persistent disturbance and delayed recovery of the endothelial cells.[4] The establishment of a functional endothelial layer soon after device implantation has been shown to be among the main factors in the prevention of restenosis and stent thrombosis.[5]

The discovery of circulating endothelial progenitor cells (EPCs)[6] opened up revolutionary new perspectives for *in vivo*/*in situ* endothelialization of implanted blood contacting biomedical devices by capturing endogenous circulating EPCs directly from the blood. Due to the promising benefits of EPCs in regenerative medicine, several molecules, such as anti-CD34 antibodies (anti-CD34 Ab), have been immobilized on the surface of devices *via* electrostatic interactions[7] or by covalent immobilization[8–10] to attract EPCs directly from the bloodstream. These methods, however, require chemical modification of the surface, and it is not possible to control the molecular orientation of the immobilized proteins. When antibodies are immobilized on a material surface, their binding activity usually decreases. This reduced binding activity is ascribed to the random orientation and steric hindrance of the antibody molecules on the material surface.[11] Therefore, a

[a]Stomatologic Hospital & College, Anhui Medical University, Key Lab. of Oral Diseases Research of Anhui Province, Hefei 230032, China. E-mail: jialong_dt@126.com; Fax: +86-551-65161183; Tel: +86-551-65161183

[b]College of Pharmacy, Anhui Medical University, Hefei 230032, China

[c]Leibniz Institute of Polymer Research Dresden, Max Bergmann Center of Biomaterials Dresden, Dresden 01069, Germany. E-mail: lijun@ahmu.edu.cn; Fax: +86-551-65161183; Tel: +86-551-65161183

method for the oriented immobilization of functional antibodies is needed.[12] Oriented immobilization of anti-CD34 Ab on materials through avidin-biotinylated protein A was described extensively by our group in a previous report and this coating could increase EPC attachment and capture, and induce rapid and complete endothelialization of the lumenal surface of the implant *in vivo*.[13] But the stability of the coating was not very good because of electrostatic interactions between the coating and material. So it is very important that anti-CD34 Ab can be tightly oriented immobilized on the material surface.

Staphylococcal protein A (SPA) is a cell wall component of the bacterium *Staphylococcus aureus* that binds specifically to many mammalian immunoglobulins, most notably immunoglobulin G (IgG), *via* the Fc region.[14] The antigen-binding capacity of antibodies linking with SPA does not interfere because the antigen-binding sites of antibodies are located on the distal ends of the Fab variable regions.[15] Thus, SPA has been used for the oriented immobilization of antibodies to retain their antigen-binding capacity in biosensors.[11]

Dopamine is a small-molecule mimic of the adhesive proteins of mussels and contains unusually high concentrations of catechol and amine functional groups, which are capable of mediating protein immobilization on most organic and inorganic surfaces.[16–19]

Inspired by this discovery as well as several successful examples of using DA and SPA in molecular immobilization, we have developed a facile approach to immobilize SPA based on surface coating of 316L SS with a thin layer of DA polymerized in the presence of SPA solution, then the SPA modified surface provided an anchor for oriented immobilization of the anti-CD34 Ab (Fig. 1).

The aim of the present study was to prepare a tight functional surface using dopamine, staphylococcal protein A and anti-CD34 Ab, and evaluate such a surface for its capacity to capture EPCs, to resist SMC attachment and to improve blood-compatibility.

2. Materials and methods

2.1 Materials

Dopamine hydrochloride, Staphylococcal Protein A (SPA), Tris–HCl buffer base and rabbit anti-goat IgG F(ab′)$_2$-peroxidase antibody were obtained from Sigma-Aldrich. Polyclonal goat anti-human-CD34 IgG and monoclonal mouse anti-human fibrinogen γ-chain were purchased from Santa cruz biotechnology Inc. and Accurate chemical & Scientific Corp., respectively. Polyclonal rabbit anti-mouse antibody against actin was purchased from Beijing Zhong Shan Golden Bridge Biological Technology CO., Ltd. Goat anti-human fibrinogen IgG HRP-conjugated antibody was purchased from Beijing Biosynthesis Biotechnology Co., Ltd. Monoclonal sheep anti-mouse IgG HRP-conjugated antibody, monoclonal mouse anti-human P-selectin antibody and monoclonal sheep anti-mouse IgG Cy3-conjugated antibody were purchased from BD Biosciences, San Jose, CA. All the other reagents used in the experiments were of the highest analytical purity (>99.9%).

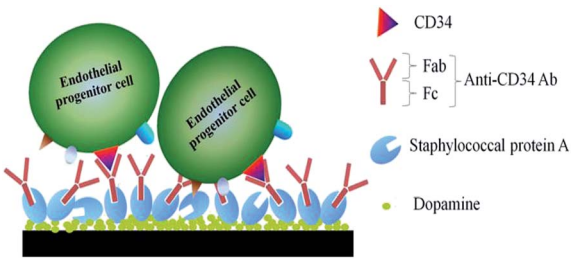

Fig. 1 Ideal reaction scheme for oriented immobilization of anti-CD34 antibodies on 316L SS through dopamine and staphylococcal protein A.

2.2 Method

2.2.1 Preparation and characterization of the modified surface. 316L SS disks were polished to a reflective mirror-like finish. The samples were ultrasonically cleaned subsequently in a detergent solution, acetone, ethanol, and finally in ultra-purified (up) water. After cleaning, the samples were immersed in a 2 mg mL^{-1} solution of dopamine (10 mM Tris buffer, pH 8.5) for about 24 h at room temperature in the dark. Then, the samples were sonicated for 10 min in up water (three times) to remove the nonattached dopamine; the samples are denoted as SS-DA. The dopamine-modified samples were then placed in a 24 well plate and incubated with a 300 μL aqueous solution of SPA (5 μg mL^{-1}) at 37 °C overnight, rinsing with up water; the samples are denoted as SS-DA-SPA. The above samples were then placed in a 24 well plate and incubated with a 300 μL aqueous solution of polyclonal goat anti-human CD34 IgG (0.1 μg mL^{-1}) at 37 °C overnight, rinsing with up water, the samples are denoted as SS-DA-SPA-CD34.

The immobilized quantity of each component was determined using a Q-Sense E4 system (Q-Sense AB, Sweden) with a fundamental frequency of 5.0 MHz. The quartz crystal microbalance (QCM) is widely used to measure the change in mass (Δm) of molecules adsorbed on the surface of the quartz crystal *via* changes in the resonance frequency (Δf). The surface of the gold (Au)-coated quartz crystal (diameter, 10 mm) was initially treated with UV irradiation for 30 min for surface cleaning and sterilizing, then placed in the measurement chamber and 10 mM Tris buffer (pH 8.5) was injected as a buffer to maintain equilibrium. A 2 mg mL^{-1} solution of dopamine (10 mM Tris buffer, pH 8.5) was injected at 10 μL min^{-1}, then rinsed with up water at 100 μL min^{-1}. Subsequently, an aqueous solution of SPA (5 μg mL^{-1}) was injected at 10 μL min^{-1} until no variation appeared in the adsorption curves, then rinsed with up water at 100 μL min^{-1}. An aqueous solution of polyclonal goat anti-human-CD34 IgG (0.1 μg mL^{-1}) was injected at 10 μL min^{-1} for building up the coating on the quartz crystal surface until no variation appeared in the adsorption curves, and then rinsed with up water at 100 μL min^{-1} for 20 min. For evaluating the stability, the coating was rinsed with up water at 500 μL min^{-1} for 24 hours. Measurements were all conducted at a temperature of 37 °C. Q-Tools software (Q-Sense AB, Gothenburg, Sweden) was used to analyze the QCM data and to extract quantitative

parameters of the adsorption of each component on the surface of the quartz crystal at the 5th overtone of the fundamental resonant frequency.

The surface composition of the samples was analyzed by X-ray photoelectron spectroscopy (XPS, Perkin Elmer 16PC) with an Al Kα X-ray source (1486.6 eV photons). A wide-scan survey spectrum over a binding energy (BE) range of 0–1400 eV was recorded at a pass energy of 80 eV for the estimation of the chemical elemental composition and 10 eV for high-resolution detailed scans. The system was calibrated using the C1s peak at 284.8 eV. All spectra were recorded at a take-off angle of 15 degree. The maximum information depth of the XPS method is not more than 10 nm. In order to determine the quantitative surface composition from XPS data, spectrum background was subtracted according to the Shirley method. The parameters of the component peak fitting were the binding energy, height, full width at half maximum, and Gaussian–Lorentzian ratio.

Water contact angle analysis was performed with a DSA100 drop shape analysis system (DSA100, Krüss, Germany) using up water at room temperature. Five samples were measured from each group, and two separate measurements were made on each sample.

The amount of F(ab′) fragments of anti-CD34 Ab exposed on the surface was determined by enzyme-linked immunosorbent assay (ELISA) as follows: (i) samples were immersed in 1% sheep serum for 60 min to block non-specific adsorption, and then the solution was decanted; (ii) 20 μm of rabbit anti-goat IgG $F(ab')_2$-peroxidase antibody (1 : 100) were added to the surface of the samples, incubated for 1 h at 37 °C, and subsequently washed with PBS for 5 min three times; (iii) 140 mL of 3,3′,5,5′-tetramethylbenzidine (TMB) chromogenic solution was added into the well containing the samples, and allowed to react for 10 min; and subsequently 200 mL of 2 M H_2SO_4 was added to stop the reaction; (vi) 150 mL of the reacting solution was transferred into a 96-well plate and was measured at 452 nm.

2.2.2 *In vitro* testing of blood compatibility

Quantification of adsorbed fibrinogen on the material surface. Fibrinogen is one of the most abundant plasma proteins (4%) and plays an important role in thrombosis.[20] So the amount of absorbed fibrinogen on the material surface was measured by direct immunochemistry.[21] Description of the procedure is presented in detail elsewhere.[10] Data are normalized to the fibrinogen adsorption to bare 316L SS as 100%.

Quantification of fibrinogen exposing γ-chains on the material surface. The conformational change of fibrinogen, *i.e.* the exposure of γ-chains (HHLGGAKQAGDV at γ 400–411), plays a critical role in fibrin cross-linking, clot formation, and interactions with other molecules.[22] The amount of exposed γ-chains on the material surfaces was measured by indirect immunochemistry.[21] Description of the procedure is presented in detail elsewhere.[10] Data are normalized to the fibrinogen exposing γ-chain to 316L SS as 100%.

Platelet adhesion testing. Platelet-rich plasma (PRP) was prepared by centrifuging (1500 rpm, 15 min) fresh human whole blood containing 3.8 wt% citrate acid solution (blood : citrate acid = 9 : 1) obtained from healthy volunteers, then 50 μL of fresh PRP was placed onto the sample surface and kept in contact with the surface for 2 h at 37 °C. After incubation, the samples were gently rinsed in PBS to remove loosely adherent platelets from the surface and then they were prepared for the subsequent SEM analysis or lactate dehydrogenase (LDH) test.

The samples were fixed with 2% glutaraldehyde in PBS for 12 h. Then the samples were washed with PBS and dehydrated in a series of increasing ethanol concentrations, then critical point dried and sputter coated with gold for observation using scanning electron microscopy.

The number of adherent platelets was quantified by determining the LDH release after lysis of the cells. A photospectrometric assay based on kinetic determination of the LDH activity was applied. The adherent platelets were lysed by the addition of 40 μL of 0.1% Triton X-100 to the sample. After 5 min incubation at room temperature (RT), 25 μL of each lysate was collected and mixed with a 200 μL mixture solution consisting of 297 μL of 10 mg mL^{-1} reduced nicotinamide adenine dinucleotide (NADH), 187 μL of 10 mg mL^{-1} pyruvate and 10 mL of tris(hydroxymethyl) aminomethane buffer, pH 7.2. The LDH activity in the lysate was then determined by recording the change in absorbance at 340 nm using a microplate photometer. This activity was related to a lysate of the platelets in the initial PRP in order to quantify the relative number of platelets on each sample.

Platelet activation: P-selectin detection. Surface-induced platelet activation was measured by the immunofluorescence method for P-selectin that is expressed on the surface of activated platelets.[23] The procedure was as follows: (i) samples with adherent platelets were fixed with 2% glutaraldehyde in PBS for 1 h and subsequently washed with PBS for 5 min; (ii) 1 mL of 1% sheep serum was added into each well and incubated for 30 min at 37 °C to block non-specific adsorption; (iii) 30 μL of monoclonal mouse anti-human antibody against P-selectin (1 : 100) was added onto the sample surfaces, incubated for 2 h at 37 °C, and subsequently washed three times with PBS for 5 min; (iv) monoclonal sheep anti-mouse IgG Cy3-conjugated antibody (1 : 100) was added to the surface of the samples, incubated for 1 h at 37 °C, and subsequently washed with PBS for 5 min three times; (v) the samples were immediately examined with a fluorescence microscope with binning 4 × 4 and an exposure time of 15 s (LEICA DMRX Polarization microscope, Leica, Germany).

2.2.3 *In vitro* testing of dynamic EPC-compatibility and SMC-compatibility

Isolation and culture of EPCs and SMCs. As previously described, mononuclear cells were separated by density gradient centrifugation (1800 rpm, 20 min) from the bone marrow of the femur of a SD rat. Mononuclear cells without further purification steps were cultured in Dulbecco's modified Eagle's medium (DMEM) (Gibco BRL, USA) containing 20% new born calf serum, 10 ng mL^{-1} VEGF, 10 ng mL^{-1} SCF, penicillin (100 U mL^{-1}), and streptomycin sulfate (100 U mL^{-1}) at 37 °C under 5% CO_2. Cells were fed with fresh medium every third day, and subcultured regularly after the adherent cells reached about 80% confluence. After 2–3 weeks of culturing under VEGF conditions, primary mononuclear cells differentiate into

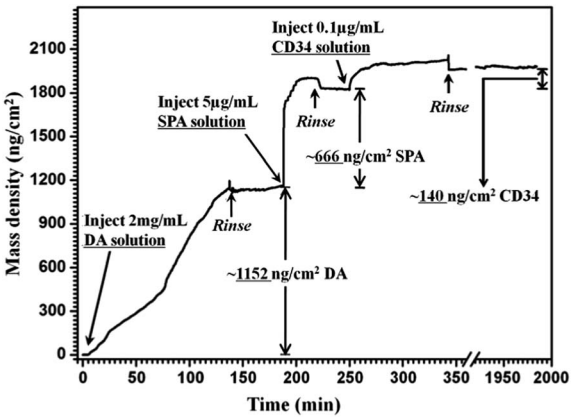

Fig. 2 Adsorbed mass changes determined from the QCM-D.

endothelial progenitor cells.[24] Human umbilical artery smooth muscle cells (SMCs) were isolated from newborn umbilical cords as described previously.[25] Cells in passages 2–5 were used. The SMCs were cultured in DMEM culture medium containing 10% new born calf serum, penicillin (100 U mL^{-1}), and streptomycin sulfate (100 U mL^{-1}) at 37 °C under 5% CO_2. Cells were fed with fresh medium every third day, and subcultured regularly after the adherent cells reached about 80% confluence.

Cell attachment of the modified surfaces under dynamic conditions in vitro. Different samples were positioned at the bottom of a parallel wall flow chamber. EPCs or SMCs were re-suspended in DMEM medium containing 10 % fetal calf serum and 50 mL of suspensions of EPCs or SMCs at a density of 1×10^6 per mL were perfused into the flow chamber at a shear rate of 1.0 Pa, similar to a small arterial flow. The parallel wall flow chamber was put into a cell incubator (at 37 °C and 5% CO_2). After 2 h or 12 h incubation, the samples were gently rinsed in PBS to remove loosely adherent cells from the surface. Then, the attached cells on the samples were determined by an MTT assay and inspected after actin expression using immunofluorescence staining.[10]

2.2.4 *In vitro* testing of macrophages compatibility. The murine macrophage cell line RAW264.7 was cultured in DMEM medium containing 10% new fetal calf serum in tissue culture polystyrene flasks. Cells were routinely detached by mechanical force and subsequently split in a ratio of 1 : 5. The samples with different surfaces were placed into the wells of a 24-well flat-bottomed plate. One milliliter of macrophage suspension at a density of 1×10^5 per mL in DMEM medium containing 10% new fetal calf serum were seeded at 37 °C for 2 h. After 2 h incubation, the samples were gently rinsed in PBS to remove loosely adherent cells from the surface. Then, the adherent macrophages on the different surfaces were analyzed for actin cytoskeleton expression using immunofluorescence staining.

2.2.5 Statistics. All experiments were performed at least three independent times. All data were compared with one-way ANOVA tests to evaluate statistical significance using SPSS software. The Tukey multiple comparison test was performed as a *post-hoc* test to find significant differences between pairs. Probability values less than 0.05 were considered statistically significant. In the figures, statistically significant differences ($p < 0.05$) were denoted by *.

2.3 Ethics statement

Fresh human whole blood and newborn umbilical cords were obtained from healthy volunteers after informed consent. All

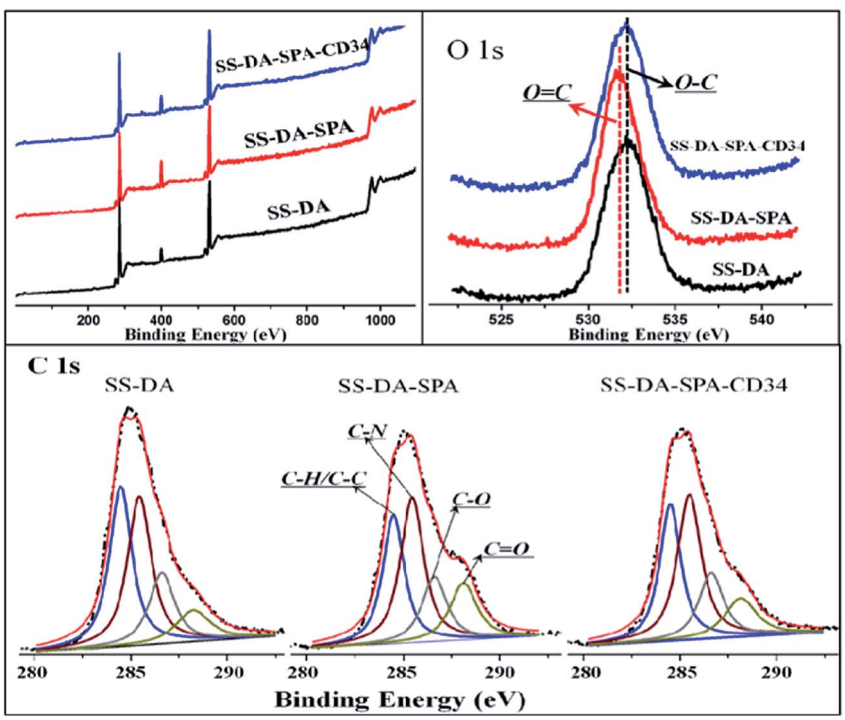

Fig. 3 The XPS spectra of different surfaces.

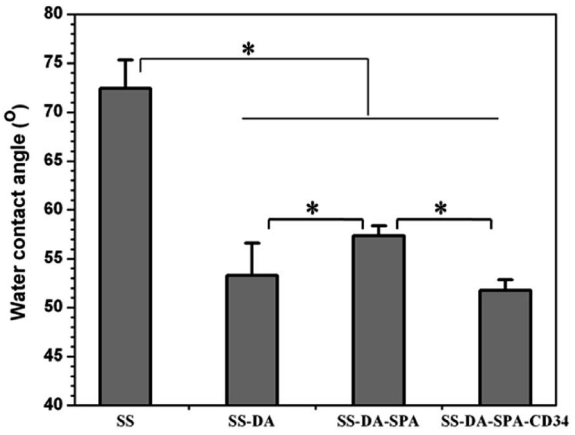

Fig. 4 Water contact angle of different surfaces.

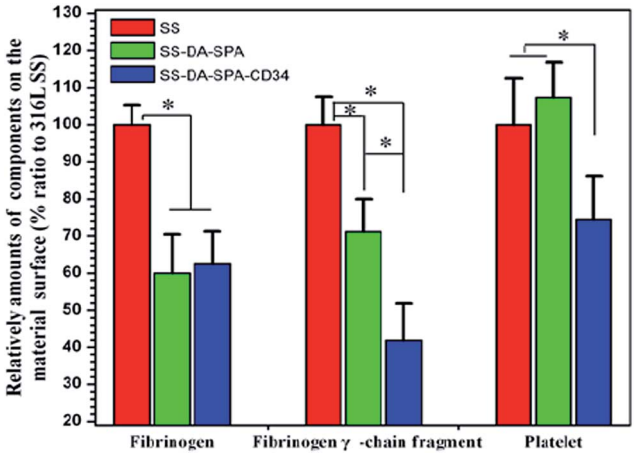

Fig. 5 Relative amount of fibrinogen, fibrinogen-exposing γ-chains, and platelets on the material surface compared with 316L SS.

animal or human subject experiments used protocols that were approved by Anhui Medical University (protocol number: 20131412).

3. Results and discussion

QCM-D has been applied to monitor the assembly process of each component on the gold-coated quartz crystal surface in real time. Mass *vs.* time curves (Fig. 2) clearly demonstrated the buildup process of the coating. Upon injection of DA or SPA or CD34 solution, the crystal frequency decreased (data not shown), indicating the adsorption of the DA or the SPA or the anti-CD34 antibody onto the crystal surface. The adsorbed amounts of DA, SPA and anti-CD34 Ab were ~1152 ng cm^{-2}, ~666 ng cm^{-2} and ~140 ng cm^{-2}, respectively as determined by Q-Tools software. Dopamine has been widely used for biomaterial surface modification, as it is easy to obtain abundant active groups (mostly phenolic hydroxyl/*o*-quinone and amino/imino) for bimolecular immobilization on the material surface with a minimal change in the chemical structure of biomaterials.[26] Here, dopamine was used to bind SPA onto substrate materials. The QCM results indicated that dopamine was successfully immobilized onto the 316L SS surface, meanwhile, dopamine adsorption on the quartz crystal surface was observed as a continuous mass increase with the deposition time and did not reach the adsorption saturation. Based on the previous studies,[27] dissolved oxygen and pH induce dihydroxyl group protons in dopamine to deprotonate, oxidizing dopamine to dopaminequinone. When the amine group is deprotonated, the molecule can undergo a 1,4 Michael addition. Further rearrangement leads to 5,6-dihydroxyindole, and further oxidation causes indolequinone formation. The reverse dismutation reaction between catechol and *o*-quinone of 5,6-dihydroxyindole leads to cross-linking and formation of polydopamine (self-polymerization), so dopamine could continuously adsorb onto materials with the deposition time. With increasing the deposition time, polydopamine would cover the substrate materials completely. Then subsequent immobilization of biomolecules would be determined using polydopamine, so the gold (Au)-coated quartz crystal could approximately exhibit the mass change on the 316L SS surface.

The reverse dismutation reaction between catechol and *o*-quinone of 5,6-dihydroxyindole can further react with amine groups for binding proteins onto the DA surface.[26] As indicated by the QCM results, this reaction was used successfully to immobilize SPA *via* the polydopamine coating by simple immersion. SPA interacts with antibodies specifically in their Fc region, which is distant from the antigen binding sites.[11,14] The QCM data indicate that the anti-CD34 antibody was successfully immobilized onto 316L SS by simple immersion. Because SPA could lead to oriented immobilization of antibodies and up water was used as the solvent and rinsing solution, the activity of anti-CD34 is expected to be maintained. The stability of the coating was the most important factor of the technique applied. After being prepared, the coating was rinsed with up water at a high flow velocity of 500 μL min^{-1} for 24 hours (Fig. 2). No significant mass change indicated that the coating was very stable.

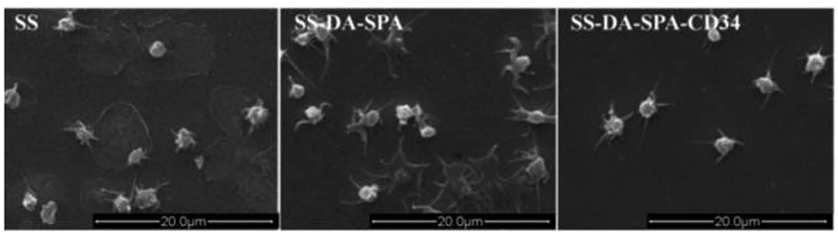

Fig. 6 SEM micrographs of platelets adhered on different surfaces.

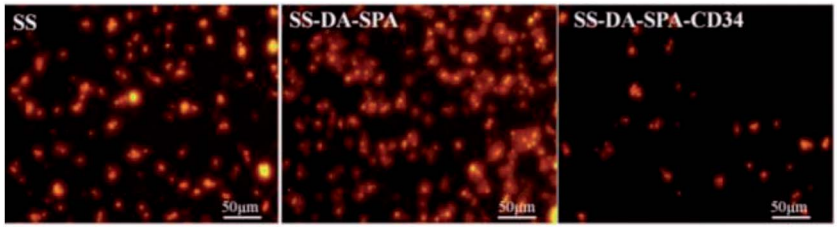

Fig. 7 Representative P-selectin stain images showing activated platelets that are labeled with a fluorescent dye.

The chemical composition of the surfaces at various stages was analyzed by XPS. The survey spectrum and high-resolution C1s and O1s spectra of the SS-DA, SS-DA-SPA and SS-DA-SPA-CD34 are represented in Fig. 3. In the survey spectrum of the SS-DA, the presence of N, which was not detected on the surface of 316L SS (data not shown) indicates that dopamine was successfully immobilized onto the surface of 316L SS. Meanwhile, Fe2p and Cr2p peaks disappeared (data not shown), indicating that dopamine had covered the substrate materials completely, so the mass change of QCM on the gold (Au)-coated quartz crystal could approximately exhibit it on the 316L SS surface.

The O1s spectra of the surfaces at various stages are shown in Fig. 3, with BEs at 531.4 eV for the O═C species and 532.9 eV for O–C species (data not shown).[26] By calculating peak areas, the molar concentration ratios of O═C/O for the SS-DA, SS-DA-SPA and SS-DA-SPA-CD34 were 38.1%, 49.5% and 44.9%, respectively. The C1s spectrum of the surfaces at various stages was curve-fitted with four peak components, with BEs at 284.5 eV for the C–C/C–H species, 285.5 eV for the C–N species, 286.6 eV for the C–O species and 288.1 eV for the C═O species.[28] By calculating peak areas, the molar concentration ratios of C═O/C for the SS-DA, SS-DA-SPA and SS-DA-SPA-CD34 were 9.9%, 16.3% and 11%, respectively. The results of O1s and C1s showed that there were more C═O species on the SPA modified surface than other surfaces. The research proved that more than 40% of the amino acid composition of SPA was Asx (asparagine and aspartate) and Glx (glutamine and glutamate) having two carbonyl groups (C═O),[29] therefore, the highest molar concentration ratios of C═O/C and O═C/O for SS-DA-SPA indicate that SPA was immobilized onto the dopamine modified surface. After anti-CD34 antibody grafting to the surface, the molar concentration ratios of C═O/C and O═C/O decreased, confirming the successful immobilization on the SPA modified surface.

The measurement of the water contact angle (WCA) is well known as a useful technique to investigate the surface characteristics. The WCA of the different surfaces is shown in Fig. 4. Compared with 316L SS, the WCA of the DA-modified surface decreased significantly. Relative to the DA-modified surface, the WCA of the SPA surface increased significantly. After anti-CD34 antibody immobilization, the WCA decreased significantly. These results indirectly indicated that three types of components were successfully immobilized onto the 316L SS surface step by step.

The amount of F(ab′) fragments of anti-CD34 Ab exposed on the surface was determined by ELISA using rabbit anti-goat IgG $F(ab')_2$-peroxidase antibody which reacts with goat IgG $F(ab')_2$ but not Fc fragments. The optical density of the anti-CD34 antibody modified surface and the SPA modified surface was measured to be 0.134 ± 0.004 and 0.010 ± 0.002, respectively. The data proved that the oriented immobilization of the anti-CD34 antibody was realized by using SPA.

Fibrinogen, one of the most important proteins in blood coagulation, has several cell adhesion and protein interaction domains. The data of fibrinogen adsorption on the various

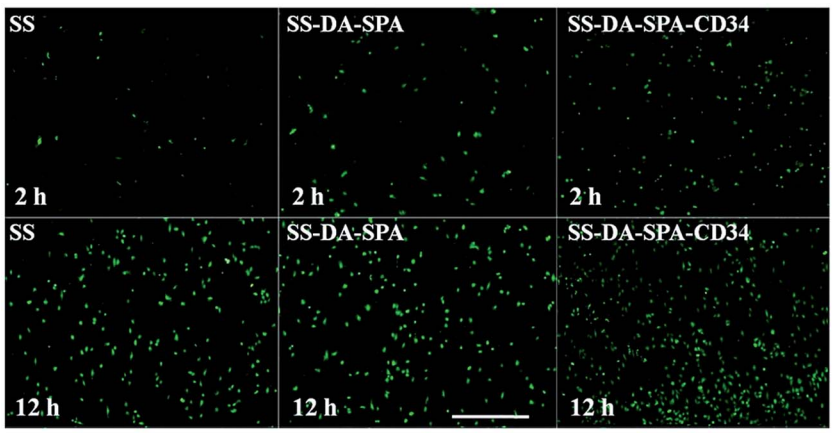

Fig. 8 FTIC-immunofluorescent micrographs of actin expression of EPCs adherent on different surfaces under flow conditions for 2 h and 12 h culture (bar 100 μm).

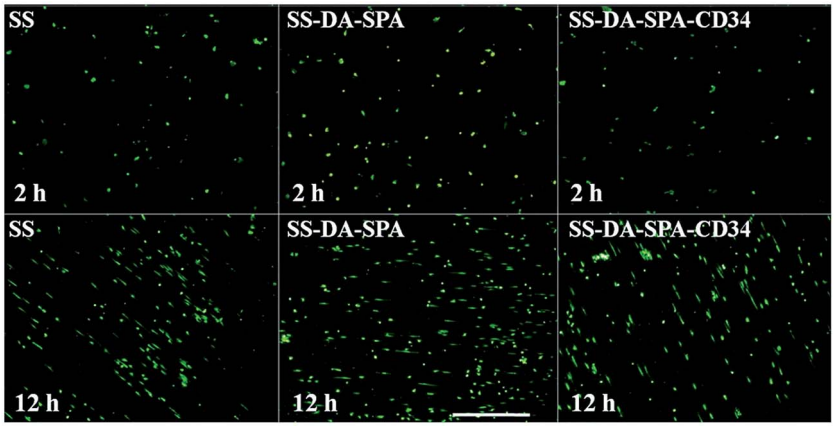

Fig. 9 FTIC-immunofluorescent micrographs of actin expression of SMCs adhered on different surfaces under flow conditions for 2 h and 12 h culture (bar 100 μm).

surfaces, normalized to the amount on 316L SS, are shown in Fig. 5. Compared to 316L SS, the amount of fibrinogen adsorbed on other surfaces decreased significantly. One reason for this may be that the hydrophilic surface could resist fibrinogen adsorption to some extent.[30] Fibrinogen adsorption onto the SPA and CD34 surface was not obviously different.

Numerous studies have demonstrated that adsorbed fibrinogen on the surface may expose previously hidden γ-chains which mediate fibrin cross-linking, clot formation, and interactions with blood platelets.[22] The relative amount of fibrinogen with exposed γ-chains on the different surfaces, normalized to the amount on 316L SS, is shown in Fig. 5. Compared to 316L SS, the amount of fibrinogen exposing γ-chains on the SPA surface significantly decreased. After anti-CD34 antibody immobilization, the amount of fibrinogen exposing γ-chains further decreased significantly.

The quantitative analysis of platelet adhesion on the different surfaces was performed, by determination of the LDH release after lysis of the adherent blood platelets. The adherent platelets on the CD34 surface were far less than on the 316L SS and SPA surface (Fig. 5), but there was no significant difference for the 316L SS and SPA surface.

SEM imaging was preformed to visualize adherent platelets on the various surfaces (Fig. 6). The largest number of adherent platelets was found on the SPA surface, while the least number was found on the CD34 surface. The platelets on the CD34 surface showed generally less pseudopodia or deformation than those on the other surfaces.

The surface-induced platelet activation was probed by fluorescence staining for P-selectin (Fig. 7); the activated platelets showed red fluorescence and were much less on the CD34 surface than on the other surfaces. The CD34 surface resisted platelet adhesion and platelet activation better than the other surfaces.

As a blood-contacting biomedical device, the surface should prevent thrombus formation. In general, when materials come into contact with blood, proteins are first adsorbed instantaneously onto the surfaces and deformed, then platelets are adsorbed, activated and aggregated. Fibrinogen is one of the most important proteins in blood coagulation. After adsorption, fibrinogen may deform to mediate thrombus formation.[22] To estimate the surface effect on fibrinogen adsorbed and fibrinogen deformed, the ratio of fibrinogen exposing γ-chains to totally adsorbed fibrinogen was used, which showed an increase in the order: SS-DA-SPA-CD34 < SS < SS-DA-SPA. The higher this ratio, the more the fibrinogen adsorbed on this surface had undergone post-adsorptive conformational changes. In protein adsorption and conformational change processes, surface chemistry is the critical determinant of the exposure of bioactive motifs that are "hidden" within the protein in its native conformation, which

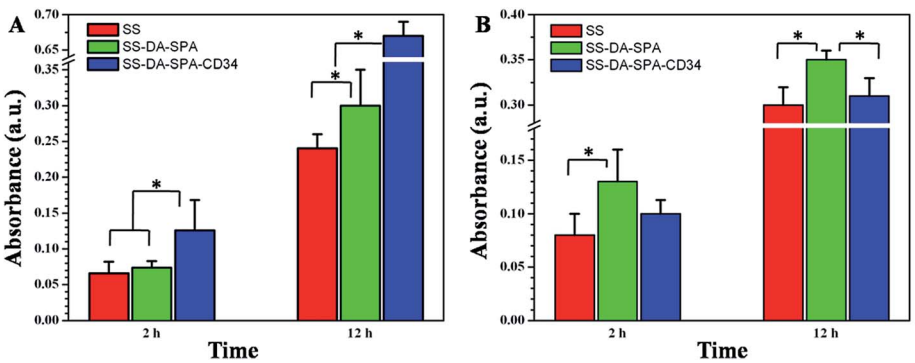

Fig. 10 EPC (A) and SMC (B) attachment on different surfaces after different culture times measured by the MTT assay. $n = 5$.

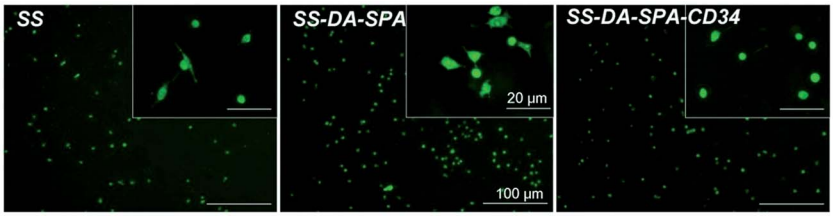

Fig. 11 FTIC-immunofluorescent micrographs of the actin cytoskeleton of macrophages adherent on different surfaces for 2 h culture.

then stimulate adverse cellular responses.[30] The results indicate that the SPA surface induces stronger conformational changes of fibrinogen than 316L SS and the CD34 surface. One reason for this may be that SS-DA-SPA has the highest molar concentration ratio of –COOH, because of more than 40% of the acidic amino acid composition of SPA.[29] A similar result was also observed in another investigation in which neutral and negative surfaces were adsorbed with equivalent amounts of fibrinogen, and the neutral surface formed little to no fibrin compared to the other surface.[31] In addition, our previous study indicated that the anti-CD34 antibody surface hinder the deformation of adsorbed fibrinogen.[10]

Platelets play a major role in the initial thrombus formation. Therefore, a study on platelet adhesion and activation is the key step to evaluate the hemocompatibility of materials. The results of the platelet adhesion test and platelet activation indicated that the CD34 surface had good hemocompatibility. One reason for this may be that the least adsorbed fibrinogen had undergone post-adsorptive conformational changes. A similar result was also observed in another investigation in which the CD34 surface had good hemocompatibility.[32]

It is known from other *in vivo* experiments that true long-term blood compatibility cannot be achieved by simply preventing platelet adhesion.[33,34] Recent studies have shown that rapid re-endothelialization at the disease site and on the surface of devices not only provides inherent antithrombogenic potential but also interrupts cytokine-driven activation of smooth muscle cells (SMCs) leading to restenosis.[5] The concept of rapid re-endothelialization has been developed to immobilize the anti-CD34 antibody with specific affinity for EPCs on a surface.[8,13,35]

In this study, the anti-CD34 antibody was immobilized onto a material surface. For the purpose of rapid re-endothelialization, the CD34 binding surface must show higher affinity for EPCs than for SMCs. To evaluate the affinity of the CD34 surface for EPCs *versus* SMCs, three types of surfaces were incubated with EPCs and SMCs under flow conditions for 2 h or 12 h. Immunofluorescent micrographs of the actin cytoskeleton show that EPCs (Fig. 8) and SMCs (Fig. 9) grew well on these surfaces. It could be seen in Fig. 9 that the number of adherent EPCs on the CD34 surface was significantly higher than on other surfaces at the initial attachment stage (2 h after seeding) and at the early growth stage (12 h after seeding), which suggested that the anti-CD34 antibody modified 316L SS favored EPC adhesion. However, no difference in adherent SMC numbers could be identified between the materials at the initial attachment stage (2 h after seeding) and at the early growth stage (12 h after seeding), which suggests that the anti-CD34 antibody modified surface did not favor SMC attachment more than other samples.

The effect of anti-CD34 antibody modification on EPC and SMC attachment is quantified at 2 h and 12 h by the MTT assay (Fig. 10). The number of adherent EPCs on the CD34 surface was about twice as many as that on the SPA surface and on the 316L SS surface after 2 h incubation. After 12 h culture, the number of adherent EPCs on the CD34 surface was far more than two-fold compared to the SPA surface and the 316L SS surface. Compared with the 316L SS surface, no significant difference of SMC attachment was observed on the CD34 surface after culturing for 2 h and 12 h. The number of adherent SMCs on the SPA surface is more than that on the other surfaces. This confirms that the CD34 surface has high affinity for EPCs rather than SMCs and is favorable for rapid re-endothelialization.

Though this anti-CD34 modified surface was unable to resist SMC attachment compared with 316L SS, it could significantly promote EPC attachment. Continuous supply of EPCs from blood could ensure that the surface was covered rapidly by EPCs, because the time needed for SMC proliferation should be longer than the time needed for EPC attachment. The clinical application of the anti-CD34-coated Genous™ Bio-engineered R stent (OrbusNeich, Hong Kong) indicated that capturing of EPCs on a surface could promote rapid re-endothelialization and inhibit SMC proliferation and thromboresistance.[36]

To study the biocompatibility of biomaterials, determining the behavior of macrophages is useful. The use of macrophages for this purpose is based on their role in the foreign body response.[37] Macrophages that adhered on the surfaces were stained for their actin cytoskeleton expression and are shown in Fig. 11. The results show that the macrophage population on the CD34 surface was significantly less than that on the SPA surface, meanwhile, macrophages extended pseudopods and frontal cytoplasmic fringes or presented an irregular shape on the 316L SS surface and the SPA surface, while less pseudopods, with an extended or rounded shape, emerged for macrophages on the CD34 surface. This implies that the CD34 surface induces lower local inflammation reaction and restenosis after implantation.

4. Conclusions

Polydopamine-staphylococcal protein A coating is an effective method for the oriented immobilization of antibodies. This was

demonstrated here with the immobilization of endothelial progenitor cell capturing anti-CD34 antibodies. Preferential binding of EPCs compared to SMCs could be observed under flow conditions, the antibody modified surface also induced less adhesion of macrophages, showing low inflammatory potential. Also other properties indicated good hemocompatibility: the surfaces adsorbed less fibrinogen compared to bare stainless steel and induced less fibrinogen denaturation than the DA-SPA surface without antibody. These properties promise a good suitability of the treatment for stent coating.

Acknowledgements

This work was supported by the Natural Science Foundation of China (no. 31300792), China Postdoctoral Science Foundation (no. 2014M561813), and the Natural Science Foundation of Anhui Province (no. 1408085QH149). This work was supported by Grants for Scientific Research of BSKY(XJ201232) from Anhui Medical University.

References

1 L. Xue and H. P. Greisler, *J. Vasc. Surg.*, 2003, **37**, 472–480.
2 C. Werner, M. F. Maitz and C. Sperling, *J. Mater. Chem.*, 2007, **17**, 3376–3384.
3 J. E. Sousa, P. W. Serruys and M. A. Costa, *Circulation*, 2003, **107**, 2274–2279.
4 D. W. Losordo, J. M. Isner and L. J. Diaz-Sandoval, *Circulation*, 2003, **107**, 2635–2637.
5 V. J. Dzau, D. Kong, L. G. Melo, A. A. Mangi, L. Zhang, M. Lopez-Ilasaca, M. A. Perrella, C. C. Liew and R. E. Pratt, *Circulation*, 2004, **109**, 1769–1775.
6 T. Asahara, T. Murohara, A. Sullivan, M. Silver, R. vanderZee, T. Li, B. Witzenbichler, G. Schatteman and J. M. Isner, *Science*, 1997, **275**, 964–967.
7 J. L. Chen, Q. L. Li, J. Y. Chen and N. Huang, *Adv. Mater. Res.*, 2008, **47–50**, 1411–1414.
8 J. Aoki, A. T. L. Ong, E. P. McFaden, W. J. van der Giessen, G. Sianos, E. Regar, P. de Feyter, M. J. B. Kutryk and P. W. Serruys, *J. Am. Coll. Cardiol.*, 2005, **45**, 69a.
9 Q. Lin, X. Ding, F. Qiu, X. Song, G. Fu and J. Ji, *Biomaterials*, 2010, **31**, 4017–4025.
10 J. Chen, J. Cao, J. Wang, M. F. Maitz, L. Guo, Y. Zhao, Q. Li, K. Xiong and N. Huang, *J. Colloid Interface Sci.*, 2012, **368**, 636–647.
11 B. Lu, M. R. Smyth and R. O'Kennedy, *Analyst*, 1996, **121**, 29R–32R.
12 C. M. Halliwell, *Analyst*, 2004, **129**, 1166–1170.
13 Q. L. Li, N. Huang, C. Chen, J. L. Chen, K. Q. Xiong, J. Y. Chen, T. X. You, J. A. Jin and X. Liang, *J. Biomed. Mater. Res., Part A*, 2010, **94**, 1283–1293.
14 N. Tajima, M. Takai and K. Ishihara, *Anal. Chem.*, 2011, **83**, 1969–1976.
15 A. P. Le Brun, S. A. Holt, D. S. Shah, C. F. Majkrzak and J. H. Lakey, *Biomaterials*, 2011, **32**, 3303–3311.
16 H. Lee, S. M. Dellatore, W. M. Miller and P. B. Messersmith, *Science*, 2007, **318**, 426–430.
17 J. G. Rivera and P. B. Messersmith, *J. Sep. Sci.*, 2012, **35**, 1514–1520.
18 D. E. Fullenkamp, J. G. Rivera, Y. K. Gong, K. H. Lau, L. He, R. Varshney and P. B. Messersmith, *Biomaterials*, 2012, **33**, 3783–3791.
19 T. S. Sileika, H. D. Kim, P. Maniak and P. B. Messersmith, *ACS Appl. Mater. Interfaces*, 2011, **3**, 4602–4610.
20 R. Murthy, C. E. Shell and M. A. Grunlan, *Biomaterials*, 2009, **30**, 2433–2439.
21 T. Y. Ning, X. H. Xu, L. F. Zhu, X. P. Zhu, C. H. Chu, L. K. Liu and Q. L. Li, *J. Biomed. Mater. Res., Part B*, 2012, **100**, 138–144.
22 M. W. Mosesson, *J. Thromb. Haemostasis*, 2003, **1**, 231–238.
23 J. L. Chen, Q. L. Li, J. Y. Chen, C. Chen and N. Huang, *Appl. Surf. Sci.*, 2009, **255**, 6894–6900.
24 J. Chen, C. Chen, Z. Chen, J. Chen, Q. Li and N. Huang, *J. Biomed. Mater. Res., Part A*, 2010, **95**, 341–349.
25 P. K. Vadiveloo, H. R. Stanton, F. W. Cochran and J. A. Hamilton, *Artery*, 1994, **21**, 161–181.
26 L. Lu, Q. L. Li, M. F. Maitz, J. L. Chen and N. Huang, *J. Biomed. Mater. Res., Part A*, 2012, **100**, 2421–2430.
27 Y. Weng, Q. Song, Y. Zhou, L. Zhang, J. Wang, J. Chen, Y. Leng, S. Li and N. Huang, *Biomaterials*, 2011, **32**, 1253–1263.
28 F. J. Xu, Q. J. Cai, Y. L. Li, E. T. Kang and K. G. Neoh, *Biomacromolecules*, 2005, **6**, 1012–1020.
29 Q. L. Li, N. Huang, J. Chen, G. Wan, A. Zhao, J. Chen, J. Wang, P. Yang and Y. Leng, *J. Biomed. Mater. Res., Part A*, 2009, **89**, 575–584.
30 B. Sivaraman, K. P. Fears and R. A. Latour, *Langmuir*, 2009, **25**, 3050–3056.
31 K. M. Evans-Nguyen, L. R. Tolles, O. V. Gorkun, S. T. Lord and M. H. Schoenfisch, *Biochemistry*, 2005, **44**, 15561–15568.
32 A. Tan, D. Goh, Y. Farhatnia, N. G., J. Lim, S. H. Teoh, J. Rajadas, M. S. Alavijeh and A. M. Seifalian, *PLoS One*, 2013, **8**, e77112.
33 M. Albers, V. M. Battistella, M. Romiti, A. A. E. Rodrigues and C. A. B. Pereira, *J. Vasc. Surg.*, 2003, **37**, 1263–1269.
34 P. Libby, M. Nahrendorf, M. J. Pittet and F. K. Swirski, *Circulation*, 2008, **117**, 3168–3170.
35 J. I. Rotmans, J. M. M. Heyligers, H. J. M. Verhagen, E. Velema, M. M. Nagtegaal, D. P. V. de Kleijn, F. G. de Groot, E. S. G. Stroes and G. Pasterkamp, *Circulation*, 2005, **112**, 12–18.
36 S. Silber, P. Damman, M. Klomp, M. A. Beijk, M. Grisold, E. E. Ribeiro, H. Suryapranata, J. Wojcik, K. Hian Sim, J. G. Tijssen and R. J. de Winter, *EuroIntervention: journal of EuroPCR in collaboration with the Working Group on Interventional Cardiology of the European Society of Cardiology*, 2011, **6**, 819–825.
37 T. Futami, N. Fujii, H. Ohnishi, N. Taguchi, H. Kusakari, H. Ohshima and T. Maeda, *J. Periodontol.*, 2000, **71**, 287–298.